
Accurate, reliable and fast robustness evaluation

Wieland Brendel^{1,3} Jonas Rauber^{1,3} Matthias Kümmerer^{1,3} Ivan Ustyuzhaninov^{1,3}

Matthias Bethge^{1,3,4}

¹Centre for Integrative Neuroscience, University of Tübingen

²International Max Planck Research School for Intelligent Systems

³Bernstein Center for Computational Neuroscience Tübingen

⁴Max Planck Institute for Biological Cybernetics

wieland.brendel@bethgelab.org

Abstract

Throughout the past five years, the susceptibility of neural networks to minimal adversarial perturbations has moved from a peculiar phenomenon to a core issue in Deep Learning. Despite much attention, however, progress towards more robust models is significantly impaired by the difficulty of evaluating the robustness of neural network models. Today’s methods are either fast but brittle (gradient-based attacks), or they are fairly reliable but slow (score- and decision-based attacks). We here develop a new set of gradient-based adversarial attacks which (a) are more reliable in the face of gradient-masking than other gradient-based attacks, (b) perform better and are more query efficient than current state-of-the-art gradient-based attacks, (c) can be flexibly adapted to a wide range of adversarial criteria and (d) require virtually no hyperparameter tuning. These findings are carefully validated across a diverse set of six different models and hold for L_2 and L_∞ in both targeted as well as untargeted scenarios. Implementations will be made available in all major toolboxes (Foolbox, CleverHans and ART). Furthermore, we will soon add additional content and experiments, including L_0 and L_1 versions of our attack as well as additional comparisons to other L_2 and L_∞ attacks¹. We hope that this class of attacks will make robustness evaluations easier and more reliable, thus contributing to more signal in the search for more robust machine learning models.

1 Introduction

Manipulating just a few pixels in an input can easily derail the predictions of a deep neural network (DNN). This susceptibility threatens deployed machine learning models and highlights a gap between human and machine perception. This phenomenon has been intensely studied since its discovery in Deep Learning [Szegedy et al., 2014] but progress has been slow [Athalye et al., 2018a].

One core issue behind this lack of progress is the shortage of tools to reliably evaluate the robustness of machine learning models. Almost all published defenses against adversarial perturbations have later been found to be ineffective [Athalye et al., 2018a]: the models just appeared robust on the surface because standard adversarial attacks failed to find the true minimal adversarial perturbations against them. State-of-the-art attacks like PGD [Madry et al., 2018] or C&W [Carlini and Wagner,

¹We expect the release of the code as well as the update of the manuscript in September 2019.

2016] may fail for a number of reasons, ranging from (1) suboptimal hyperparameters over (2) an insufficient number of optimization steps to (3) masking of the backpropagated gradients.

In this paper, we adopt ideas from the decision-based boundary attack [Brendel et al., 2018] and combine them with gradient-based estimates of the boundary. The resulting class of gradient-based attacks surpasses current state-of-the-art methods in terms of attack success, query efficiency and reliability. Like the decision-based boundary attack, but unlike existing gradient-based attacks, our attacks start from a point far away from the clean input and follow the boundary between the adversarial and non-adversarial region towards the clean input, Figure 1 (middle). This approach has several advantages: first, we always stay close to the decision boundary of the model, the most likely region to feature reliable gradient information. Second, instead of minimizing some surrogate loss (e.g. a weighted combination of the cross-entropy and the distance loss), we can formulate a clean quadratic optimization problem. Its solution relies on the local plane of the boundary to estimate the optimal step towards the clean input under the given L_p norm and the pixel bounds, see Figure 1 (right). Third, because we always stay close to the boundary, our method features only a single hyperparameter (the trust region) but no other trade-off parameters as in C&W or a fixed L_p norm ball as in PGD. We tested our attacks against the current state-of-the-art in the L_2 and L_∞ metric on two conditions (targeted and untargeted) on six different models across three different data sets. To make all comparisons as fair as possible, we conducted a large-scale hyperparameter tuning for each attack. In all cases tested, we find that our attacks outperform the current state-of-the-art in terms of attack success, query efficiency and robustness to suboptimal hyperparameter settings. We hope that these improvements will facilitate progress towards robust machine learning models.

2 Related work

Gradient-based attacks are the most widely used tools to evaluate model robustness due to their efficiency and success rate relative to other classes of attacks with less model information (like decision-based, score-based or transfer-based attacks, see [Brendel et al., 2018]). This class includes many of the best-known attacks such as L-BFGS [Szegedy et al., 2014], FGSM [Goodfellow et al., 2015], JSMA [Papernot et al., 2016], DeepFool [Moosavi-Dezfooli et al., 2016], PGD [Kurakin et al., 2016, Madry et al., 2018], C&W [Carlini and Wagner, 2016], EAD [Chen et al., 2017] and SparseFool [Modas et al., 2019]. Nowadays, the two most important ones are PGD with a random starting point [Madry et al., 2018] and C&W [Carlini and Wagner, 2016]. They are usually considered the state of the art for L_∞ (PGD) and L_2 (CW). The other ones are either much weaker (FGSM, DeepFool) or minimize other norms, e.g. L_0 (JSMA, SparseFool) or L_1 (EAD).

More recently, there have been some improvements to PGD that aim at making it more effective and/or more query-efficient by changing its update rule to Adam [Uesato et al., 2018] or momentum [Dong et al., 2018]. Initial comparisons to these attacks (not shown) do not suggest any changes in our conclusions w.r.t. to our results on L_∞ but we will add a full comparison in the next version of the manuscript.

3 Attack algorithm

Our attacks are inspired by the decision-based boundary attack [Brendel et al., 2018] but use gradients to estimate the local boundary between adversarial and non-adversarial inputs. We will refer to this boundary as the *adversarial boundary* for the rest of this manuscript. In a nutshell, the attack starts from an adversarial input \tilde{x}^0 (which may be far away from the clean sample) and then follows the adversarial boundary towards the clean input x , see Figure 1 (middle). To compute the optimal step in each iteration, Figure 1 (right), we solve a quadratic trust region optimization problem. The goal of this optimization problem is to find a step δ^k such that (1) the updated perturbation $\tilde{x}^k = \tilde{x}^{k-1} + \delta^k$ has a smaller L_p distance to the clean input x , (2) the size $\|\delta^k\|_2^2$ of the step is smaller than a given trust region radius r , (3) the updated perturbation stays within the box-constraints of the valid input value range (e.g. $[0, 1]$ or $[0, 255]$ for input) and (4) the updated perturbation \tilde{x}^k is approximately placed on the adversarial boundary.

Optimization problem In mathematical terms, this optimization problem can be phrased as

$$\min_{\delta} \|x - \tilde{x}^{k-1} - \delta\|_p \quad \text{s.t.} \quad 0 \leq \tilde{x}^{k-1} + \delta \leq 1 \quad \wedge \quad \mathbf{b}^{k\top} \delta = c^k \quad \wedge \quad \|\delta\|_2^2 \leq r, \quad (1)$$

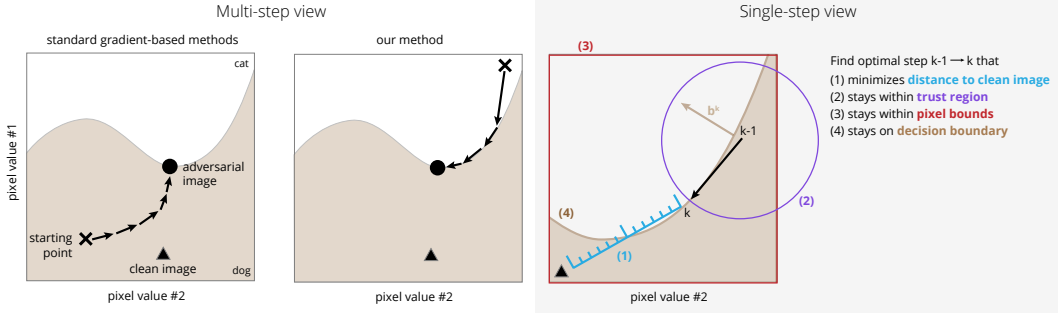


Figure 1: Schematic of our approach. Consider a two-pixel input which a model either interprets as a *dog* (shaded region) or as a *cat* (white region). Given a clean image (solid triangle), we search for the closest image classified as a *cat*. Standard gradient-based attacks start somewhere near the clean image and perform gradient descent towards the boundary (left). Our attacks start from an adversarial image far away from the clean image and walk along the boundary towards the closest adversarial (middle). In each step, we solve an optimization problem to find the optimal descent direction along the boundary that stays within the valid pixel bounds and the trust region (right).

where $\|\cdot\|_p$ denotes the L_p norm and \mathbf{b}^k denotes the estimate of the normal vector of the local boundary (see Figure 1) around $\tilde{\mathbf{x}}^{k-1}$ (see below for details). For L_2 , Eq. (1) is a quadratically-constrained quadratic program (QCQP) while for L_∞ , it is straight-forward to write Equation (1) as a linear program with quadratic constraints (LPQC), see the supplementary material. Both problems can be solved with off-the-shelf solvers like ECOS [Domahidi et al., 2013] or SCS [O’Donoghue et al., 2016] but the runtime of these solvers as well as their numerical instabilities in high dimensions prohibits their use in practice. We therefore derived efficient iterative algorithms to solve Eq. (1) for L_2 and L_∞ . The additional optimization step has little to no impact on the runtime of our attack compared to standard iterative gradient-based attacks like PGD. We report the details of the derivation and the resulting algorithms in the supplements.

For L_2 , the algorithm to solve Equation (1) is basically an active-set method: in each iteration, we first ignore the pixel bounds, solve the residual QCQP analytically, and then project the solution back into the pixel bounds. In practice, the algorithm converges after a few iterations to the optimal solution δ_k .

For L_∞ , we note that the optimization problem in Eq. (1) can be reduced to the L_2 problem for a fixed L_∞ norm of size ϵ . We then perform a simple and fast binary search to minimize ϵ .

Adversarial criterion Our attacks move along the adversarial boundary to minimize the distance to the clean input. We assume that this boundary can be defined by a differentiable equality constraint $\text{adv}(\tilde{\mathbf{x}}) = 0$, i.e. the manifold that defines the boundary is given by the set of inputs $\{\tilde{\mathbf{x}} \mid \text{adv}(\tilde{\mathbf{x}}) = 0\}$. No other assumptions about the adversarial boundary are being made. Common choices for $\text{adv}(\cdot)$ are targeted or untargeted adversarials, defined by perturbations that switch the model prediction from the ground-truth label y to either a specified target label t (targeted scenario) or any other label $t \neq y$ (untargeted scenario). More precisely, let $\mathbf{m}(\tilde{\mathbf{x}}) \in \mathbb{R}^C$ be the class-conditional log-probabilities predicted by model $\mathbf{m}(\cdot)$ on the input $\tilde{\mathbf{x}}$. Then $\text{adv}(\tilde{\mathbf{x}}) = \mathbf{m}(\tilde{\mathbf{x}})_y - \mathbf{m}(\tilde{\mathbf{x}})_t$ is the criterion for targeted adversarials and $\text{adv}(\tilde{\mathbf{x}}) = \min_{t, t \neq y} (\mathbf{m}_y(\tilde{\mathbf{x}}) - \mathbf{m}_t(\tilde{\mathbf{x}}))$ for untargeted adversarials.

The direction of the boundary \mathbf{b}^k in step k at point $\tilde{\mathbf{x}}^{k-1}$ is defined as the derivative of $\text{adv}(\cdot)$,

$$\mathbf{b}^k = \nabla_{\tilde{\mathbf{x}}^{k-1}} \text{adv}(\tilde{\mathbf{x}}^{k-1}). \quad (2)$$

Hence, any step δ^k for which $\mathbf{b}^{k\top} \delta^k = \text{adv}(\tilde{\mathbf{x}}^{k-1})$ will move the perturbation $\tilde{\mathbf{x}}^k = \tilde{\mathbf{x}}^{k-1} + \delta^k$ onto the adversarial boundary (if the linearity assumption holds exactly). In Eq. (1), we defined $c^k \equiv \text{adv}(\tilde{\mathbf{x}}^{k-1})$ for brevity. Finally, we note that in the targeted and untargeted scenarios, we compute gradients for the same loss found to be most effective in Carlini and Wagner [2016]. In our case, this loss is naturally derived from a geometric perspective of the adversarial boundary.

Starting point The algorithm always starts from a point $\tilde{\mathbf{x}}^0$ that is typically far away from the clean image and lies in the adversarial region. There are several straight-forward ways to find such

starting points, e.g. by (1) sampling random noise inputs, (2) choosing a real sample that is part of the adversarial region (e.g. is classified as a given target class) or (3) choosing the output of another adversarial attack.

In all experiments presented in this paper, we choose the starting point as the closest sample (in terms of the L_2 norm) to the clean input which was classified differently (in untargeted settings) or classified as the desired target class (in targeted settings) by the given model. After finding a suitable starting point, we perform a binary search with a maximum of 10 steps between the clean input and the starting point to find the adversarial boundary. From this point, we perform an iterative descent along the boundary towards the clean input. Algorithm 1 provides a compact summary of the attack procedure.

Algorithm 1: Schematic of our attacks.

Data: clean input x , differentiable adversarial criterion $\text{adv}(\cdot)$, adversarial starting point \tilde{x}^0

Result: adversarial example \tilde{x} such that the distance $d(x, \tilde{x}^k) = \|x - \tilde{x}^k\|_p$ is minimized

begin

$k \leftarrow 0$

$\mathbf{b}^0 \leftarrow \mathbf{0}$

 if no \tilde{x}^0 is given: $\tilde{x}^0 \sim \mathcal{U}(0, 1)$ s.t. \tilde{x}^0 is adversarial (or sample from adv. class)

while $k < \text{maximum number of steps}$ **do**

$\mathbf{b}^k := \nabla_{\tilde{x}^{k-1}} \text{adv}(\tilde{x}^{k-1})$ // estimate local geometry of decision boundary

$c^k := \text{adv}(\tilde{x}^{k-1})$ // estimate distance to decision boundary

$\delta^k \leftarrow$ solve optimization problem Eq. (1) for given L_p norm

$\tilde{x}^k \leftarrow \tilde{x}^{k-1} + \delta^k$

$k \leftarrow k + 1$

end

end

4 Methods

We extensively compare the proposed attack against current state-of-the-art attacks in a range of different scenarios. This includes six different models (varying in model architecture, defense mechanism and data set), two different adversarial categories (targeted and untargeted) and two different metrics (L_2 and L_∞). In addition, we perform a large-scale hyperparameter tuning for all attacks we compare against in order to be as fair as possible. The full analysis pipeline is built on top of *Foolbox* [Rauber et al., 2017] and will be published soon.

Attacks We compare against the two attacks which are considered to be the current state-of-the-art in L_2 and L_∞ according to the recently published guidelines [Carlini et al., 2019]:

- *Projected Gradient Descent (PGD)* [Madry et al., 2018]. Iterative gradient attack that optimizes L_∞ by minimizing a cross-entropy loss under a fixed L_∞ norm constraint enforced in each step.
- *C&W* [Carlini and Wagner, 2016]. L_2 iterative gradient attack that relies on the Adam optimizer, a tanh-nonlinearity to respect pixel-constraints and a loss function that weighs a classification loss with the distance metric to be minimized.

Models We test all attacks on all models regardless as to whether the models have been specifically defended against the distance metric the attacks are optimizing. The sole goal is to evaluate all attacks on a maximally broad set of different models to ensure their wide applicability. For all models, we used the official implementations of the authors as available in the *Foolbox model zoo* [Rauber et al., 2017].

- *Madry-MNIST* [Madry et al., 2018]: Adversarially trained model on MNIST. Claim: 89.62% (L_∞ perturbation ≤ 0.3). Best third-party evaluation: 88.42% [Wang et al., 2018].

- *Madry-CIFAR* [Madry et al., 2018]: Adversarially trained model on CIFAR-10. Claim: 47.04% (L_∞ perturbation $\leq 8/255$). Best third-party evaluation: 44.71% [Zheng et al., 2018].
- *Distillation* [Papernot et al., 2015]: Defense (MNIST) with increased softmax temperature. Claim: 99.06% (L_0 perturbation ≤ 112). Best third-party evaluation: 3.6% [Carlini and Wagner, 2016].
- *Logitpairing* [Kannan et al., 2018]: Variant of adversarial training on downscaled ImageNET (64 x 64 pixels) using the logit vector instead of cross-entropy. Claim: 27.9% (L_∞ perturbation $\leq 16/255$). Best third-party evaluation: 0.6% [Engstrom et al., 2018].
- *Kolter & Wong* [Kolter and Wong, 2017]: Provable defense that considers a convex outer approximation of the possible hidden activations within an L_p ball to optimize a worst-case adversarial loss over this region. MNIST claims: 94.2% (L_∞ perturbations ≤ 0.1).
- *ResNet-50* [He et al., 2016]: Standard vanilla ResNet-50 model trained on ImageNET that reaches 50% for L_2 perturbations $\leq 1 \times 10^{-7}$ [Brendel et al., 2018].

Adversarial categories We test all attacks in two common attack scenarios: *untargeted* and *targeted* attacks. In other words, perturbed inputs are classified as adversarials if they are classified differently from the ground-truth label (untargeted) or are classified as a given target class (targeted).

Hyperparameter tuning We ran PGD, C&W and our attacks on each model/attack combination and each sample with five repetitions and eight different hyperparameter settings. For each attack, we only varied the step sizes and left all other hyperparameters constant. We tested $[1 \times 10^{-6}, 1 \times 10^{-5}, 1 \times 10^{-4}, 1 \times 10^{-3}, 1 \times 10^{-2}, 1 \times 10^{-1}, 1, 2]$ for PGD, $[1 \times 10^{-4}, 1 \times 10^{-3}, 3 \times 10^{-3}, 1 \times 10^{-2}, 3 \times 10^{-2}, 1 \times 10^{-1}, 3 \times 10^{-7}, 1]$ for C&W and $[3 \times 10^{-4}, 1 \times 10^{-3}, 3 \times 10^{-3}, 1 \times 10^{-2}, 3 \times 10^{-2}, 1 \times 10^{-1}, 3 \times 10^{-1}, 1]$ for our attacks. For C&W, we set the number of steps to 200 and binary search steps to 9. All other hyperparameters were left at their default values².

Evaluation The success of an L_∞ attack is typically quantified as the *attack success rate* within a given L_∞ norm ball. In other words, the attack is allowed to perturb the clean input with a maximum L_∞ norm of ϵ and one measures the classification accuracy of the model on the perturbed inputs. The smaller the classification accuracy the better performed the attack. PGD [Madry et al., 2018], the current state-of-the-art attack on L_∞ , is highly adapted to this scenario and expects ϵ as an input.

This contrasts with most L_2 attacks like C&W [Carlini and Wagner, 2016] which are designed to find minimal adversarial perturbations. In such scenarios, it is more natural to measure the success of an attack as the median over the adversarial perturbation sizes across all tested samples [Schott et al., 2019]. The smaller the median perturbations the better the attack.

Our attacks also seek minimal adversarials and thus lend themselves to both evaluation schemes. To make the comparison to the current state-of-the-art as fair as possible, we adopt the success rate criterion on L_∞ and the median perturbation distance on L_2 .

All results reported have been evaluated on 1000 validation samples³. For the L_∞ evaluation, we chose ϵ for each model and each attack scenario such that the best attack performance reaches roughly 50% accuracy. This makes it easier to compare the performance of different attacks (compared to thresholds at which model accuracy is close to zero or close to clean performance). In the untargeted scenario, we chose $\epsilon = 0.33, 0.15, 0.1, 0.03, 0.0015, 0.0006$ in the untargeted and $\epsilon = 0.35, 0.2, 0.15, 0.06, 0.04, 0.002$ in the targeted scenarios for *Madry-MNIST*, *Kolter & Wong*, *Distillation*, *Madry-CIFAR*, *Logitpairing* and *ResNet-50*, respectively.

²In the next update of the manuscript we additionally optimize C&W over its initial tradeoff-constant. Our preliminary results on this, however, do not show any substantial differences to the results presented here.

³Except for the results on ResNet-50, which have been run on 100 samples due to time-constraints. We will report the full results in the next version of the paper.

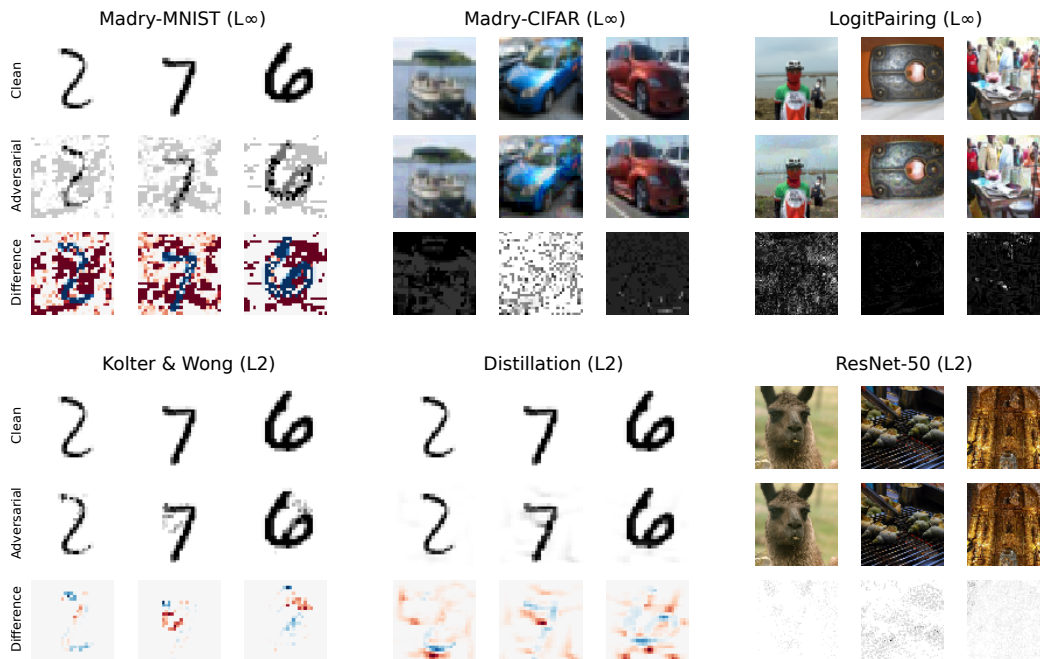


Figure 2: Randomly selected adversarial examples found by our attacks for each model. The top part shows adversarial examples that minimize the L_∞ norm while the bottom row shows adversarial examples that minimize the L_2 norm.

5 Results

5.1 Attack success

In both targeted as well as untargeted attack scenarios, our attacks surpass the current state-of-the-art on every single model we tested, see Table 1 (untargeted) and Table 2 (targeted). While the gains are small on some models like *Distillation* or *Madry-CIFAR*, we reach quite substantial gains on others: on *Madry-MNIST*, our untargeted L_2 attack reaches median perturbation sizes of 1.15 compared to 3.46 for C&W. In the targeted scenario, the difference is even more pronounced (1.70 vs 5.15). On L_∞ , our attack further reduces the model accuracy by 0.1% to 9.1% relative to PGD. Adversarial examples produced by our attacks are visualized in Figure 2.

	MNIST			CIFAR-10	ImageNet	
	<i>Madry-MNIST</i>	<i>K&W</i>	<i>Distillation</i>	<i>Madry-CIFAR</i>	<i>LP</i>	<i>ResNet-50</i>
PGD	59.3%	74.5%	30.3%	49.9%	24.1%	53%
Ours- L_∞	50.2%	68.4%	29.6%	49.8%	19.3%	41%
C&W	3.46	2.87	1.10	0.76	0.10	0.15
Ours- L_2	1.15	1.62	1.07	0.72	0.09	0.13

Table 1: **Attack success in untargeted scenario.** Model accuracies (PGD and Ours- L_∞) and median perturbation distance (C&W and Ours- L_2) in *untargeted* attack scenarios. Smaller is better.

	MNIST			CIFAR-10	ImageNet	
	<i>Madry-MNIST</i>	<i>K&W</i>	<i>Distillation</i>	<i>Madry-CIFAR</i>	<i>LP</i>	<i>ResNet-50</i>
PGD	65.5%	46.3%	52.8%	39.1%	1.5%	47%
Ours- L_∞	57.7%	38.7%	50.1%	37.3%	0.6%	42%
C&W	5.15	4.21	2.10	1.21	0.54	0.46
Ours- L_2	1.70	2.32	2.06	1.16	0.52	0.4

Table 2: **Attack success in targeted scenario.** Model accuracies (PGD and Ours- L_∞) and median adversarial perturbation distance (C&W and Ours- L_2) in *targeted* attack scenarios. Smaller is better.

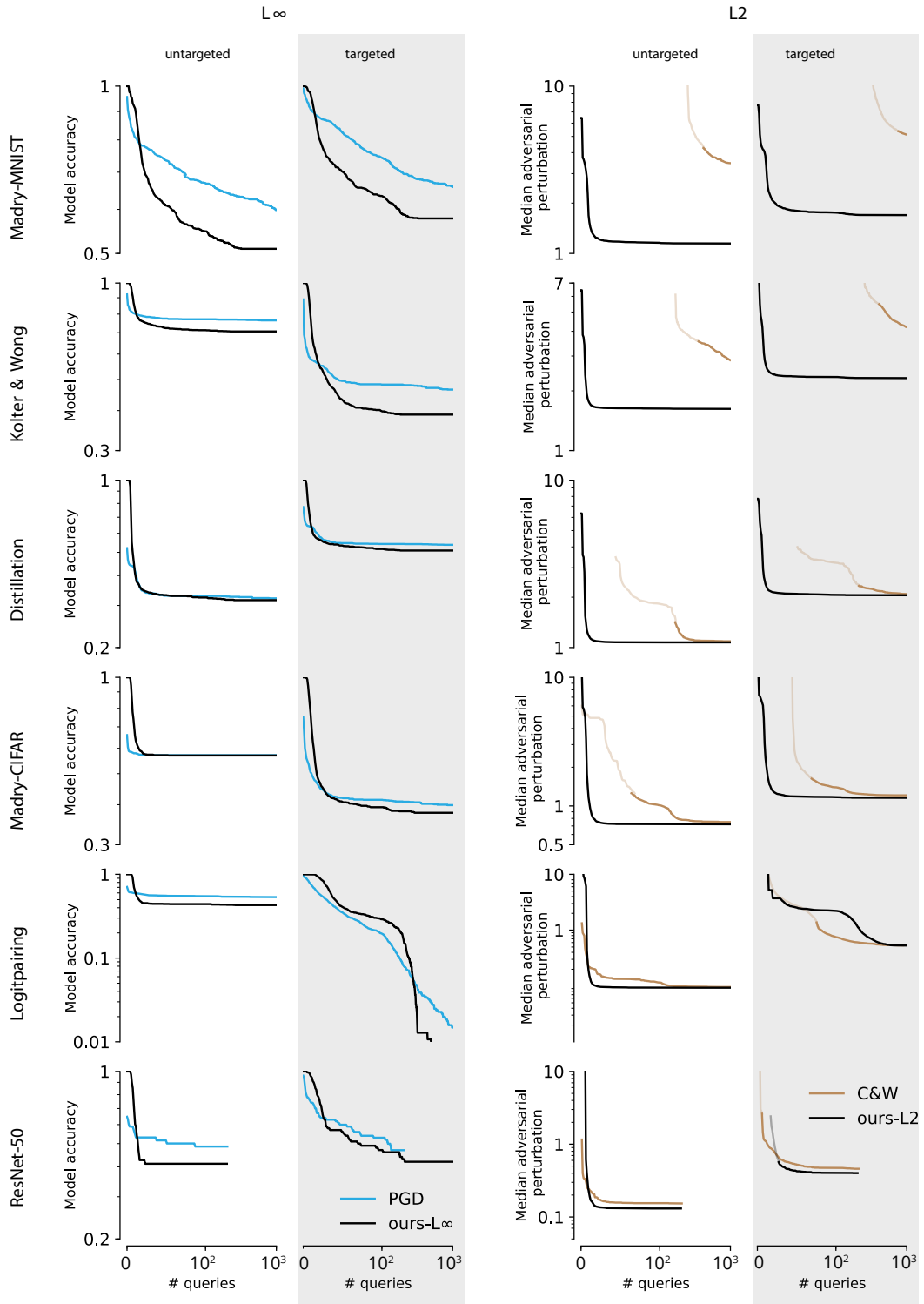


Figure 3: Query-Success curves for all model/attack combinations in the targeted and untargeted scenario. Each curve shows the attack success either in terms of model accuracy (for L_∞ , left part) or median adversarial perturbation size (for L_2 , right part) over the number of queries to the model. In both cases, lower is better. For each point on the curve, we selected the optimal hyperparameter.

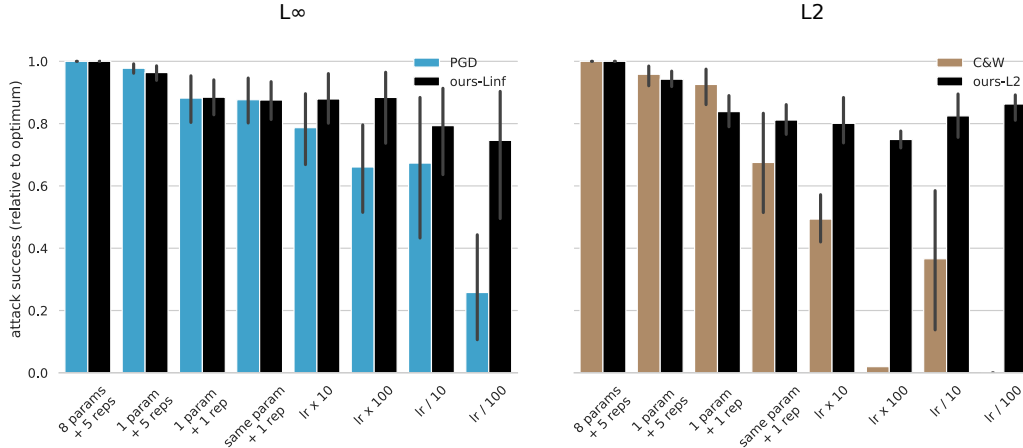


Figure 4: Sensitivity of our method to the number of repetitions and suboptimal hyperparameters.

5.2 Query efficiency

On L_2 , our attack is drastically more query efficient than C&W, see the query-distortion curves in Figure 3. Each curve represents the maximal attack success (either in terms of model accuracy or median perturbation size) as a function of query budget. For each query (i.e. each point of the curve) and each model, we select the optimal hyperparameter. This ensures that we tease out how good each attack can perform in limited-query scenarios. We find that our L_2 attack generally requires only about 10 to 20 queries to get close to convergence while C&W often needs several hundred iterations.

Similarly, our L_∞ attack generally surpasses PGD in terms of attack success after around 10 queries. The first few queries are typically required by our attack to find a suitable point on the adversarial boundary. This gives PGD a slight advantage at the very beginning.

5.3 Hyperparameter robustness

In Figure 4, we show the results of an ablation study. In the full case ($8\ params + 5\ reps$), we run all attacks with all eight hyperparameter values and with five repetitions for 1000 steps on each sample and model. We then choose the smallest adversarial input across all hyperparameter values and all repetitions. This is the baseline we compare all ablations against. The results are as follows:

- Like PGD or C&W, our attacks experience only a 4% performance drop if a single hyperparameter is used instead of eight.
- Our attacks experience around 15% - 19% drop in performance for a single hyperparameter and only one instead of five repetitions, similar to PGD and C&W.
- We can even choose the same trust region hyperparameter across all models with no further drop in performance. C&W, in comparison, experiences a further 16% drop in performance, meaning it is more sensitive to per-model hyperparameter tuning.
- Our attack is extremely insensitive to suboptimal hyperparameter tuning: changing the optimal trust region two orders of magnitude up or down changes performance by less than 15%. In comparison, just one order of magnitude deteriorates C&W performance by almost 50%. Larger deviations from the optimal learning rate disarm C&W completely. PGD is less sensitive than C&W but still experiences large drops if the learning rate gets too small.

6 Discussion & Conclusion

An important obstacle slowing down the search for robust machine learning models is the lack of reliable evaluation tools: out of roughly two hundred defenses proposed and evaluated in the literature, less than a handful are widely accepted as being effective. A more reliable evaluation of adversarial

robustness has the potential to more clearly distinguish effective defenses from ineffective ones, thus providing more signal and thereby accelerating progress towards robust models.

In this paper, we introduced a novel class of gradient-based attacks that outperforms the current state-of-the-art in terms of attack success, query efficiency and reliability on L_2 and L_∞ . By moving along the adversarial boundary, our attacks stay in a region with fairly reliable gradient information. Other methods like C&W which move through regions far away from the boundary might get stuck due to obfuscated gradients, a common issue for robustness evaluation [Athalye et al., 2018b].

Further extensions to other L_p metrics like L_1 are possible as long as the optimization problem Eq. (1) can be solved efficiently. We are currently working on an extension towards L_1 and L_0 which we will add in the next iteration of the manuscript. Extensions to other adversarial criteria are trivial as long as the boundary between the adversarial and the non-adversarial region can be described by a differentiable equality constraint. This makes the attack more suitable to scenarios other than targeted or untargeted classification tasks.

Taken together, our methods set a new standard for adversarial attacks that is useful for practitioners and researchers alike to find more robust machine learning models.

Acknowledgments

This work has been funded, in part, by the German Federal Ministry of Education and Research (BMBF) through the Bernstein Computational Neuroscience Program Tübingen (FKZ: 01GQ1002) as well as the German Research Foundation (DFG CRC 1233 on “Robust Vision”) and the BMBF competence center for machine learning (FKZ 01IS18039A). The authors thank the International Max Planck Research School for Intelligent Systems (IMPRS-IS) for supporting J.R., M.K. and I.U.; J.R. acknowledges support by the Bosch Forschungsstiftung (Stifterverband, T113/30057/17); M.B. acknowledges support by the Centre for Integrative Neuroscience Tübingen (EXC 307); W.B. and M.B. were supported by the Intelligence Advanced Research Projects Activity (IARPA) via Department of Interior / Interior Business Center (DoI/IBC) contract number D16PC00003.

References

- Anish Athalye, Nicholas Carlini, and David A. Wagner. Obfuscated gradients give a false sense of security: Circumventing defenses to adversarial examples. *CoRR*, abs/1802.00420, 2018a. URL <http://arxiv.org/abs/1802.00420>.
- Anish Athalye, Nicholas Carlini, and David A. Wagner. Obfuscated gradients give a false sense of security: Circumventing defenses to adversarial examples. *CoRR*, abs/1802.00420, 2018b. URL <http://arxiv.org/abs/1802.00420>.
- W. Brendel, J. Rauber, and M. Bethge. Decision-based adversarial attacks: Reliable attacks against black-box machine learning models. In *International Conference on Learning Representations*, 2018. URL <https://arxiv.org/abs/1712.04248>.
- Nicholas Carlini and David A. Wagner. Towards evaluating the robustness of neural networks. *CoRR*, abs/1608.04644, 2016. URL <http://arxiv.org/abs/1608.04644>.
- Nicholas Carlini, Anish Athalye, Nicolas Papernot, Wieland Brendel, Jonas Rauber, Dimitris Tsipras, Ian J. Goodfellow, Aleksander Madry, and Alexey Kurakin. On evaluating adversarial robustness. *CoRR*, abs/1902.06705, 2019. URL <http://arxiv.org/abs/1902.06705>.
- Pin-Yu Chen, Yash Sharma, Huan Zhang, Jinfeng Yi, and Cho-Jui Hsieh. Ead: elastic-net attacks to deep neural networks via adversarial examples. *arXiv preprint arXiv:1709.04114*, 2017.
- Alexander Domahidi, Eric Chun-Pu Chu, and Stephen P. Boyd. Ecos: An socp solver for embedded systems. *2013 European Control Conference (ECC)*, pages 3071–3076, 2013.
- Yinpeng Dong, Fangzhou Liao, Tianyu Pang, Hang Su, Jun Zhu, Xiaolin Hu, and Jianguo Li. Boosting adversarial attacks with momentum. In *Proceedings of the IEEE Conference on Computer Vision and Pattern Recognition*, 2018.

- Logan Engstrom, Andrew Ilyas, and Anish Athalye. Evaluating and understanding the robustness of adversarial logit pairing. *CoRR*, abs/1807.10272, 2018. URL <http://arxiv.org/abs/1807.10272>.
- Ian Goodfellow, Jonathon Shlens, and Christian Szegedy. Explaining and harnessing adversarial examples. In *International Conference on Learning Representations*, 2015. URL <http://arxiv.org/abs/1412.6572>.
- Kaiming He, Xiangyu Zhang, Shaoqing Ren, and Jian Sun. Deep residual learning for image recognition. In *2016 IEEE Conference on Computer Vision and Pattern Recognition, CVPR 2016, Las Vegas, NV, USA, June 27-30, 2016*, pages 770–778, 2016. doi: 10.1109/CVPR.2016.90. URL <https://doi.org/10.1109/CVPR.2016.90>.
- Harini Kannan, Alexey Kurakin, and Ian J. Goodfellow. Adversarial logit pairing. *CoRR*, abs/1803.06373, 2018. URL <http://arxiv.org/abs/1803.06373>.
- J. Zico Kolter and Eric Wong. Provable defenses against adversarial examples via the convex outer adversarial polytope. *CoRR*, abs/1711.00851, 2017. URL <http://arxiv.org/abs/1711.00851>.
- Alexey Kurakin, Ian Goodfellow, and Samy Bengio. Adversarial examples in the physical world. *arXiv preprint arXiv:1607.02533*, 2016.
- Aleksander Madry, Aleksandar Makelov, Ludwig Schmidt, Dimitris Tsipras, and Adrian Vladu. Towards deep learning models resistant to adversarial attacks. In *6th International Conference on Learning Representations, ICLR 2018, Vancouver, BC, Canada, April 30 - May 3, 2018, Conference Track Proceedings*, 2018. URL <https://openreview.net/forum?id=rJzIBfZAb>.
- Apostolos Modas, Seyed-Mohsen Moosavi-Dezfooli, and Pascal Frossard. Sparsefool: a few pixels make a big difference. In *The IEEE Conference on Computer Vision and Pattern Recognition (CVPR)*, 2019.
- Seyed-Mohsen Moosavi-Dezfooli, Alhussein Fawzi, and Pascal Frossard. Deepfool: A simple and accurate method to fool deep neural networks. In *The IEEE Conference on Computer Vision and Pattern Recognition (CVPR)*, June 2016.
- B. O’Donoghue, E. Chu, N. Parikh, and S. Boyd. Conic optimization via operator splitting and homogeneous self-dual embedding. *Journal of Optimization Theory and Applications*, 169(3): 1042–1068, June 2016. URL <http://stanford.edu/~boyd/papers/scs.html>.
- Nicolas Papernot, Patrick D. McDaniel, Xi Wu, Somesh Jha, and Ananthram Swami. Distillation as a defense to adversarial perturbations against deep neural networks. *CoRR*, abs/1511.04508, 2015. URL <http://arxiv.org/abs/1511.04508>.
- Nicolas Papernot, Patrick McDaniel, Somesh Jha, Matt Fredrikson, Z Berkay Celik, and Ananthram Swami. The limitations of deep learning in adversarial settings. In *Security and Privacy (EuroS&P), 2016 IEEE European Symposium on*, pages 372–387. IEEE, 2016.
- Jonas Rauber, Wieland Brendel, and Matthias Bethge. Foolbox v0.8.0: A python toolbox to benchmark the robustness of machine learning models. *CoRR*, abs/1707.04131, 2017. URL <http://arxiv.org/abs/1707.04131>.
- Lukas Schott, Jonas Rauber, Matthias Bethge, and Wieland Brendel. Towards the first adversarially robust neural network model on MNIST. In *International Conference on Learning Representations*, 2019. URL <https://openreview.net/forum?id=S1EH0sC9tX>.
- Christian Szegedy, Wojciech Zaremba, Ilya Sutskever, Joan Bruna, Dumitru Erhan, Ian Goodfellow, and Rob Fergus. Intriguing properties of neural networks. In *International Conference on Learning Representations*, 2014. URL <http://arxiv.org/abs/1312.6199>.
- Jonathan Uesato, Brendan O’Donoghue, Aaron van den Oord, and Pushmeet Kohli. Adversarial risk and the dangers of evaluating against weak attacks. *arXiv preprint arXiv:1802.05666*, 2018.

Shiqi Wang, Yizheng Chen, Ahmed Abdou, and Suman Jana. Mixtrain: Scalable training of formally robust neural networks. *arXiv preprint arXiv:1811.02625*, 2018.

Tianhang Zheng, Changyou Chen, and Kui Ren. Distributionally adversarial attack. *CoRR*, abs/1808.05537, 2018. URL <http://arxiv.org/abs/1808.05537>.